energies

MDPI

Article

Characteristics of Wind Resources and Post-Project Evaluation of Wind Farms in Coastal Areas of Zhejiang

Guangyu Fan [1,2], Yanru Wang [2,3,*], Bo Yang [1], Chuanxiong Zhang [3], Bin Fu [2] and Qianqian Qi [4]

[1] School of Civil Engineering and Architecture, Zhejiang SCI-TECH University, Hangzhou 310018, China; fgyzjlg@163.com (G.F.); youngbo@zstu.edu.cn (B.Y.)
[2] School of Civil Engineering, Taizhou University, Taizhou 317000, China; dorofubin@tzc.edu.cn
[3] Key Laboratory of Intelligent Lifeline Protection and Emergency Technology for Resident ATY, Wenzhou University of Technology, Wenzhou 150080, China; zhangcx@wzu.edu.cn
[4] State Key Laboratory of Mountain Bridge and Tunnel Engineering, Chongqing Jiaotong University, Chongqing 400074, China; 622200970065@mails.cqjtu.edu.cn
* Correspondence: yanrupiaoyang@163.com

Abstract: As the onshore wind farm technology matures, offshore wind energy has attracted increasing attention. Zhejiang has coastal areas with massive potential for wind resources because of its geographical location. Therefore, understanding the wind resources in these areas can lay a foundation for future development and utilization. On this basis, this study used the measured wind field data of a wind farm along the coast of Zhejiang from March 2014 to February 2015 and from March 2016 to February 2018 to investigate and compare the characteristics of wind energy resources, including average wind speed, Weibull shape and scale factors, wind direction variation, and wind energy density. Then, the capacity coefficient of a wind turbine predicted using the wind farm data was compared with the actual capacity coefficients of two wind turbines in the wind farm in 2019. Results revealed the following observations: The overall variations in the evaluation indicators followed clear patterns over the 3 years. For example, the main wind direction in the same season was the same, and the variations in the monthly average wind speed, the monthly wind power density, and the theoretical capacity factors were highly similar. The time-series data indicated that the difference in the indicators between summer and autumn was significantly larger than that between other seasons, with the maximum difference in monthly average wind speed of 1.46 times and the maximum difference in monthly wind power density of 1.5 times. The comparison results of the capacity coefficient showed that the theoretical and actual capacity coefficients were extremely close when the monthly average wind speed was less than 6 m/s, with the average difference being less than 9%. When the monthly average wind speed was greater than 6 m/s, the proximity between the theoretical and actual capacity coefficients was reduced, with an average difference of more than 9% and a maximum value of 28%. In general, the overall characteristics of wind resources in coastal areas of Zhejiang exhibited similar trends but fluctuated considerably in some months. Wind energy forecasts had significant discrepancies from the actual operation indicators of the wind farm when the wind speed was high.

Keywords: wind energy characteristics; Weibull distribution; wind power density; wind farm; capacity factor; post-project evaluation

Citation: Fan, G.; Wang, Y.; Yang, B.; Zhang, C.; Fu, B.; Qi, Q. Characteristics of Wind Resources and Post-Project Evaluation of Wind Farms in Coastal Areas of Zhejiang. *Energies* **2022**, *15*, 3351. https://doi.org/10.3390/en15093351

Academic Editor: Eugen Rusu

Received: 11 April 2022
Accepted: 2 May 2022
Published: 4 May 2022

1. Introduction

The energy shortage problem has become a key issue in the sustainable development of various countries. Given its wide application, low cost, and sustainability, wind energy has gradually become one of the indispensable renewable energy sources in the world [1]. Therefore, as an alternative energy source, wind energy has been vigorously promoted in many countries, both on land and in the oceans [2]. In the last 10 years, globally installed wind energy capacity has increased from 198 GW in 2010 to 841.9 GW in 2021, i.e., an

increase of 4.25 times [3,4]. China has vast amounts of land and a long coastline, providing it with abundant onshore and offshore wind energy resources [5]; thus, the utilization of wind energy in China is expanding. In accordance with the domestic wind power industry statistics, the cumulative installed capacity of wind power in the country was 328 GW by the end of 2021, among which the cumulative installed capacity of onshore wind power was 302 GW, and that of offshore wind power was about 26.3 GW [6]. These data indicate that the importance of wind energy has been generally recognized, particularly in recent years, and many countries worldwide have become aware of low-carbon environmental protection. This scenario will further increase the utilization rate of wind energy.

The development of onshore wind energy resources has finally reached maturity at present, and development has begun to move gradually toward nearshore and ocean regions. Chen [7] conducted a comprehensive statistical analysis of the wind energy potential in the northern coastal area of Beibu Gulf by using the meteorological observation data of seven islands. The results showed that the wind energy resources in this area are rich and worthy of vigorous development. Shu [8] conducted a statistical analysis of wind characteristics and energy resources on the basis of the wind data of five weather stations in Hong Kong under different terrain conditions. He concluded that wind energy density in mountaintop and offshore areas is significantly higher than that in urban areas. Emeksiz [9] conducted research and analysis on the potential of offshore wind energy in Turkey and selected areas suitable for installing offshore wind farms in the country. Many studies have also evaluated marine or coastal wind energy resources in different regions [10,11]; all of these studies have concluded that abundant wind energy resources are available. Zhejiang Province is bounded by the East China Sea to the east and has a coastline of 3200 km. It has a subtropical monsoon climate with prominent monsoons and is endowed with substantial offshore wind resources. China has been vigorously exploiting offshore wind resources. Table 1 introduces seven wind farms under planning and construction; their completion can effectively alleviate energy shortages [12]. Table 1 shows that the offshore wind resources in the coastal areas of Zhejiang will be further exploited in the future. An accurate understanding of the wind resource characteristics in the coastal areas of Zhejiang provides a reference for wind farms currently under construction and plays an essential role in guiding future exploitation of wind resources.

Table 1. Progress plan of key wind power projects in Zhejiang.

Project Name	Project Scale	Total Project Investment (Unit: Ten Thousand RMB)	Planned Construction Duration
National Xiangshan No. 1 Offshore Wind Farm	Installed capacity: 0.2542 GW	429,518	2020–2022
Huaneng Cangnan No. 4 Offshore Wind Power Project	Installed capacity: 0.2542 GW	872,150	2020–2024
Huarun Cangnan No. 1 Offshore Wind Power Project	Installed capacity: 0.4 GW	620,000	2020–2023
Huaneng Jiaxing Offshore Wind Power Project	Installed capacity: 0.402 GW	531,400	2019–2022
Zheneng Jiaxing No. 1 Offshore Wind Power Project	Installed capacity: 0.3 GW	558,225	2019–2021
Huadian Yuhuan No. 1 Offshore Wind Farm	Installed capacity: 0.3 GW	505,747	2019–2022
CSIC Haizhuang Xiangshan Offshore Wind Power Project	Installed capacity: 1.2 GW	1,020,000	2020–2023

The first step to understanding wind resources is analyzing the characteristics of wind parameters at a given location. A probability distribution model of wind speed that fits the disordered and random wind speed data are often necessary to facilitate the calculation of a series of measurable parameters. The probability distribution function is a method used by scholars and experts to evaluate wind resources [13]. In general, the probability

distribution of wind speed is a skewed normal distribution; the wind speed distribution models include the Weibull distribution model, the Rayleigh distribution model, and the log-normal distribution model [14–16]. H.Saleh [17], Manwell [18], Li [19], and Sant'Anna de Sousa Gomes [20] used the Weibull distribution to evaluate wind resources in a certain area. They concluded that the Weibull distribution is the most suitable for evaluating wind resources. Many methods for estimating the shape parameters of Weibull distribution of wind speed are available. Different methods can be adopted for different available wind speed data. The most commonly used methods are the graphical method, method of moments, power density method, and maximum likelihood estimation method [21–24]. Many scholars compared different Weibull distribution parameter estimation methods. They concluded that the maximum likelihood estimation method is the best solution at present. For example, Khalid Saeed [25] adopted six methods to evaluate wind resources in northern Pakistan and believed that the maximum likelihood estimation method is the most effective. Tizgui [26] used seven methods to calculate the Weibull distribution parameters and concluded that the maximum likelihood estimation method has the minimum error. Ouahabi [27] also used different methods to calculate the Weibull distribution parameters and came to the same conclusion. Therefore, the maximum likelihood estimation method was used to calculate the parameters in this study. Many scholars have proposed new methods, including the fourth-order hybrid method by Sumair [28], the cross-entropy method by Wan [29], and the artificial intelligence optimization method based on the Chebyshev metric by Abid Saeed [30], to determine the Weibull distribution parameters. However, these methods have not been widely used because of their complexity and limited applicability.

The post-project evaluation of a wind farm project refers to the systematic and objective evaluation of the project's operation after the project is completed and put into operation for a certain period. The post-project evaluation provides experience and lessons for future project decision making to achieve optimal control of investment projects. Many existing studies adopted the capacity factor to measure the potential energy output of wind turbines in a region. For example, Li [31] analyzed the wind data collected at 10 min intervals from three locations near the shoreline of Lake Erie to evaluate the characteristics of wind resources and estimated the capacity factor of wind turbines at hub heights of 50 and 80 m using two commercial wind turbines. Khahro [32] calculated the wind power density and wind speed frequency distribution at four different heights in a wind farm in southern Pakistan and predicted the energy output through the capacity factor of wind turbines. Carreno-Madinabeitia [33] analyzed the temporal and spatial variations in offshore wind power density and capacity factors around the Iberian Peninsula during the 20th century. However, most of the previous studies merely used the capacity factor to predict the amount of wind's output energy. The researchers of these studies failed to recognize that predicting this amount aims to improve the use of wind resources in the region. Whether the wind farm can generate the predicted amount of energy during its actual operation needs further research. Thus, in this study, the capacity factor was used to evaluate the actual operational efficiency of a specific wind farm along the coast of Zhejiang to determine whether the wind farm has achieved its expected energy generation target.

In this study, the importance of wind resources in the coastal areas of Zhejiang was considered, multiyear wind farm data and operational data of wind turbines were analyzed, the characteristics of wind resources in these areas were determined, and a post-project evaluation of wind farm projects was carried out. The characteristics of wind resources help in understanding the wind power utilization in this area, thereby providing a reference for the future development and utilization of wind energy in coastal areas. The comparison between the predicted amount of output energy and the actual operation of wind power plants can provide a reference for improving wind energy prediction methods. The post-project evaluation can shed light on wind farm site selection and the improvement of wind energy prediction methods. Figure 1 details the main workflow of this study.

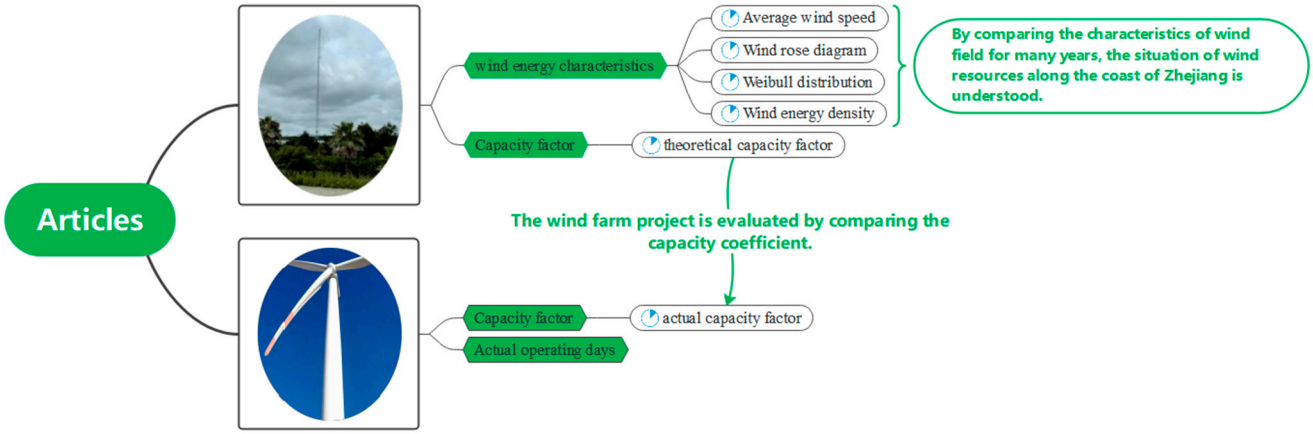

Figure 1. Main workflow of this study.

2. Analysis Method

2.1. Average Wind Speed

Wind changes over time, such as diurnally and monthly. Therefore, wind exhibits different volatility characteristics at varying time scales [34]. Average wind speed is generally used to study this variation law. Average wind speed is the average value of the instantaneous wind speed at a given time, with the given time varying from a few seconds to several years. The average wind speed (V) is calculated as follows [35]:

$$V = \frac{1}{n}\sum_{n=1}^{n} V_i, \tag{1}$$

where V_i is the wind speed (m/s) observation sequence, and n is the number of wind speed sequences in an average wind speed calculation period.

2.2. Weibull Distribution

Wind speed is highly random, and its statistical characteristics can be approximately described by fitting a probability model of wind speed distribution [36]. These models can achieve good results in some cases; among them, the Weibull distribution model works the best. The probability density and cumulative distribution functions of the Weibull distribution are as follows [37]:

$$f(v) = \frac{k}{c}\left(\frac{v}{c}\right)^{k-1} e^{-(v/c)^k}, \tag{2}$$

$$F(v) = 1 - exp\left[-\left(\frac{v}{c}\right)^k\right], \tag{3}$$

where v is wind speed (m/s); k is the shape parameter of the Weibull distribution, dimensionless; c is the scale parameter of the Weibull distribution (m/s). In the current study, the MLE method is used to solve the Weibull parameter. The formula for calculating the Weibull parameter by using the MLE method is as follows [37]:

$$k = \left(\frac{\sum_{i=1}^{N} v_i^k ln(v_i)}{\sum_{i=1}^{N} v_i^k} - \frac{\sum_{i=1}^{N} ln(v_i)}{N}\right)^{-1}, \tag{4}$$

$$c = \left(\frac{1}{N}\sum_{i=1}^{N} v_i^k\right)^{1/k}, \tag{5}$$

where v_i is the average wind speed at a certain time, and N is the number of nonzero wind speeds.

2.3. Wind Power Density

Wind power density, also known as wind energy density, refers to the wind energy that the airflow vertically passes through a unit cross-sectional area in a unit of time [38]. When the wind power density in a certain area is higher, the wind energy resources in that area are better, and the wind energy utilization rate is higher. Wind power density is an important parameter in wind energy resource assessment, and its calculation method is as follows [39]:

$$p(v) = \int_0^\infty \frac{P(v)}{A} f(v)dv = \int_0^\infty \frac{1}{2}\rho c^3 f(v)dv = \frac{1}{2}\rho c^3 \Gamma\left(1 + \frac{3}{k}\right), \quad (6)$$

$$\Gamma(x) = \int_0^\infty e^{-u} u^{x-1} du, \quad (7)$$

where *P(v)* is the wind energy (W); *p(v)* is the unit of wind power density (W/m^2); ρ is the air density and typically 1.255 kg/m^3. A is the rotating area of the wind turbine blade, and $\Gamma(x)$ is the gamma function.

2.4. Predicted Power Generation and Capacity Factor

To better evaluate the potential of wind energy resources in a region, a specific type of wind turbine is usually used to calculate wind *EO*. For a given wind turbine, *EO* is calculated as follows [40]:

$$EO = N \int_{v_{ct}}^{v_{co}} p_t(v) f(v) dv, \quad (8)$$

where *EO* is the power generation of the wind turbine at a certain period, *N* is the time to calculate power generation (h), *Vco* is the cut-out wind speed of the wind turbine, *Vct* is the cut-in wind speed of the wind turbine, and $p_t(v)$ is the power output curve of the actual wind turbine.

The capacity factor is one of the major performance indicators in wind farm projects. It is usually defined as the ratio of the predicted power generation to the rated capacity. The capacity factor depends on the parameters and performance of the wind turbine and the characteristics of wind resources [41]. Many studies have shown that the larger the capacity factor is, the higher the utilization rate of wind energy is. Therefore, the capacity factor is one of the standards for wind turbine performance evaluation. It is also an indispensable part of the post-project evaluation of wind farms. The capacity factor is calculated as follows [40]:

$$C_f = \frac{EO}{N \times P_r}, \quad (9)$$

$$C_{fd} = C_{ft} - C_{fa}, \quad (10)$$

where N is the abovementioned time when the electricity generation is calculated, *Pr* is the rated power of the wind turbine, C_{fd} is the difference between the theoretical and the actual capacity factor, C_{ft} is the theoretical capacity factor, and C_{fa} is the actual capacity factor.

3. Location Description

3.1. Research Site

This study used the wind measurement tower data of a coastal wind farm located in Wenling, Zhejiang Province. This wind farm is distributed in a long and narrow strip, with a length of about 5 km from north to south and a width of about 1 km to 3 km from east to west. Twenty 2000 kW horizontal axis wind turbines are arranged in a single row along the embankment. As shown in Figure 2, the wind measuring tower is located between F3 and F4 wind turbines. Figure 3 shows an actual photograph of the wind measuring tower.

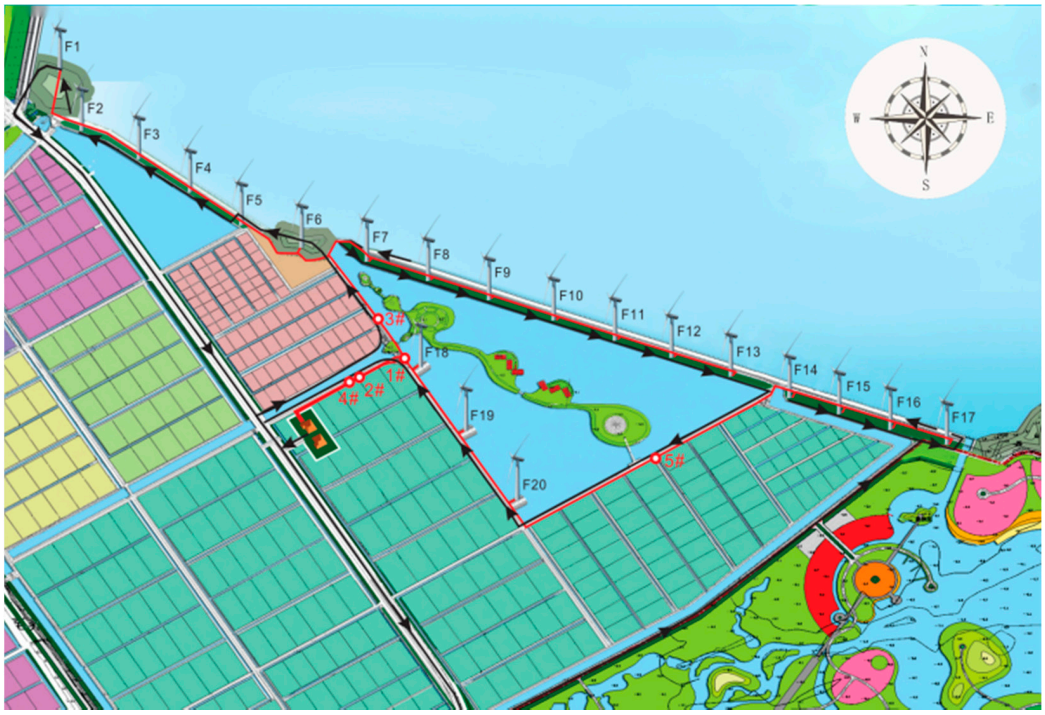

Figure 2. Wind farm.

Figure 3. Wind measuring tower.

Located on the East China Sea coast, this area features coastal mudflats and has a coastline of approximately 4.5 km. It starts from Shangmeng Mountain in the north and ends at Hengqi Mountain in the south. It has a subtropical monsoon climate. Under the influence of the marine climate, the temperature and pressure gradients between the sea routes are large, and the sea breeze and land breeze are prominent. It is also a typhoon-prone area; thus, it is affected by extreme weather events, such as strong winds and typhoons in summer and autumn every year. Sometimes, severe typhoons make a direct landfall. Consequently, wind speed and direction data fluctuate considerably. Accordingly, this study used wind field data for three years to study the changes in characteristics of wind resources in the coastal areas of Zhejiang.

3.2. Equipment

The data in this study derive from wind field data collected by an anemometer placed 70 m above the ground on the anemometer tower. Although the anemometer tower is located between the F3 and F4 wind turbines, it is approximately 100 m away from either wind turbine. The prevailing winds in this wind farm blow from the north and the southwest, which happen to be perpendicular to the wind turbine configuration. Therefore, the wind turbines have little impact on the anemometer placed on the tower. The anemometer is an ultrasonic anemometer produced by the British FT Company. The model is FT702LT-V22-FF, as shown in Figure 4. The anemometer measures data every 10 min by the resonance of the ultrasonic signal in its own measuring cavity. For clarity, the three periods, March 2014–February 2015, April 2016–February 2017, and March 2017–February 2018, are hereinafter represented as Year 2014, Year 2016, and Year 2017, respectively.

Figure 4. FT702LT-V22-FF anemometer.

For this research, the power generation data of two wind turbines in the region in 2019 and over 1 year of operation were selected. The model of the two wind turbines is Vestas® V80, and they have been operating normally at the wind farm. Table 2 provides the parameters of the wind turbine, including the rated power of 2000 kW, a cut-in wind speed of 3.5 m/s, and a cut-out wind speed of 25 m/s. Figure 5 presents a power curve diagram of the two wind turbines.

Table 2. Parameters of the wind turbines.

Performance	Description
Model	Vestas® V80
Rated power	2000 KW
Number of blades	3
Rotor diameter	80 m
Cut-in wind speed	3.5 m/s
Cut-out wind speed	25 m/s
Rated wind speed	13 m/s
Hub height	67 m

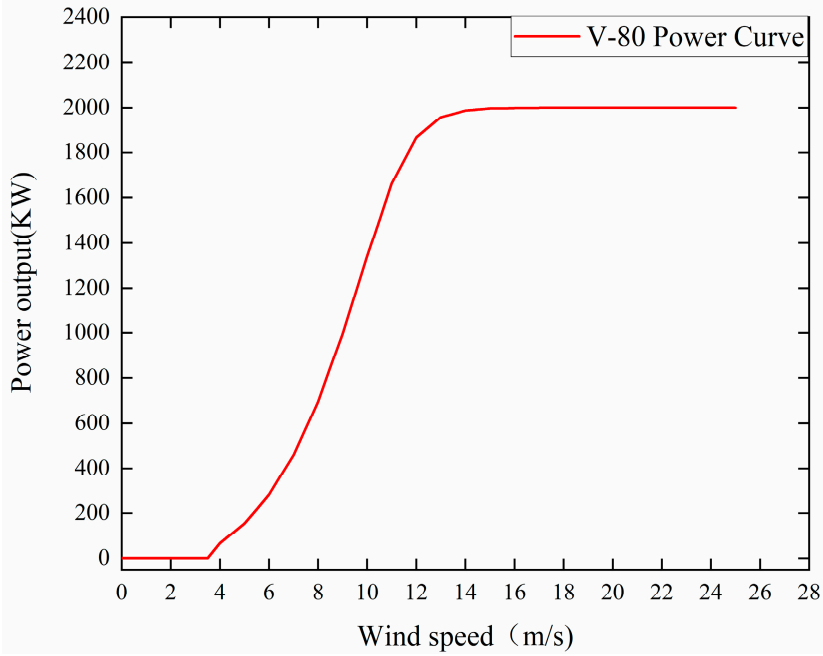

Figure 5. Power curve of the wind turbines.

4. Data Analysis

4.1. Average Wind Speed

The monthly variation in the average wind speed can visually display the size and variation trends of wind speed among different months. Figure 6 shows the 3-year monthly average wind speed variation in the coastal area of Taizhou. As shown in the figure, the overall changing trend of monthly average wind speed in this area was the same. The average wind speeds in May were the smallest, with values of 4.15, 4.54, and 4.20 m/s; the average wind speeds in July and October were the largest, with values of 5.69, 6.84, and 6.80 m/s; the average wind speeds in October were 5.4, 6.85, and 7.87 m/s. Meanwhile, the monthly average wind speed in summer and autumn was larger than that in other seasons and exhibited obvious seasonal changes. The characteristics of seasonal fluctuations were found through the comparison of monthly average wind speed over 3 years. The changing range of monthly average wind speed was small in spring and winter, and the changing range of monthly average wind speed was large in summer and autumn, especially in October 2017, when it was 1.46 times higher than that in October 2014. The coastal areas are affected by complex weather. The average wind speed was larger in summer and autumn, but the difference among different years was also large, and the maximum multiple was 1.46 times.

4.2. Wind Rose Diagram

A wind rose diagram is an important parameter for wind resource assessment. It is drawn by wind speed and the corresponding wind direction. It mostly provides useful information, such as the frequency of the dominant wind direction and speed in different directions. On the basis of the average wind speed and wind direction data every 10 min for 3 years, the rose map of wind direction for each season in the region is plotted in Figure 7, for 3 years. The figure shows that the dominant wind direction was different in each season, but the dominant wind direction was roughly the same in the same season in different years. In spring, the dominant wind direction in 3 years was SSW, with frequencies of 15.2%, 18.2%, and 14.8%, respectively. In summer, the dominant wind direction in 3 years became SSW, and the frequency was more than 20%, especially in 2016, when it was 41%. Therefore, the dominant wind direction in summer is particularly suitable for the utilization of wind energy resources. The dominant wind direction was similar in autumn and winter.

The dominant wind direction in 3 years was concentrated in NNW, N, and NNE, and the frequency of the three directions was very close. Specifically, in autumn 2016, the frequency rates of the three directions were 16.2%, 17.2%, and 17.2%, respectively. The prevailing winds in this area blow from the north and the southwest, which happen to be perpendicular to the configuration of wind turbines. Thus, the prevailing winds facilitate the operation of wind farms.

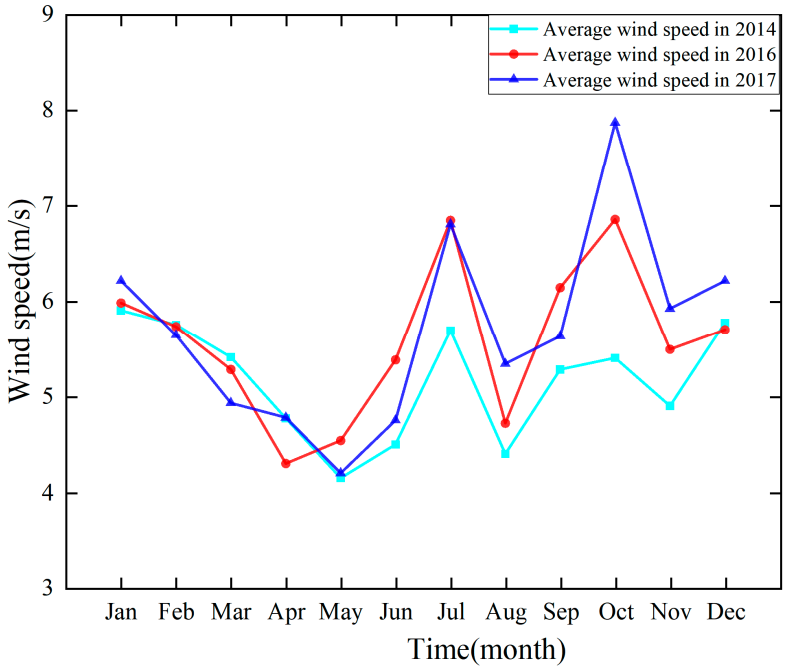

Figure 6. Average monthly wind speed over 3 years.

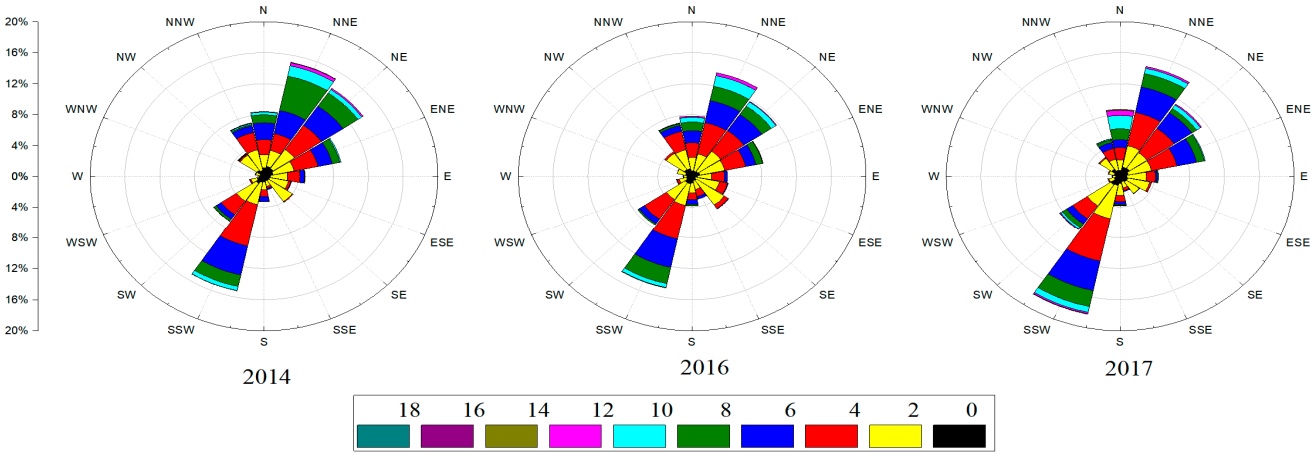

(**a**)

Figure 7. *Cont.*

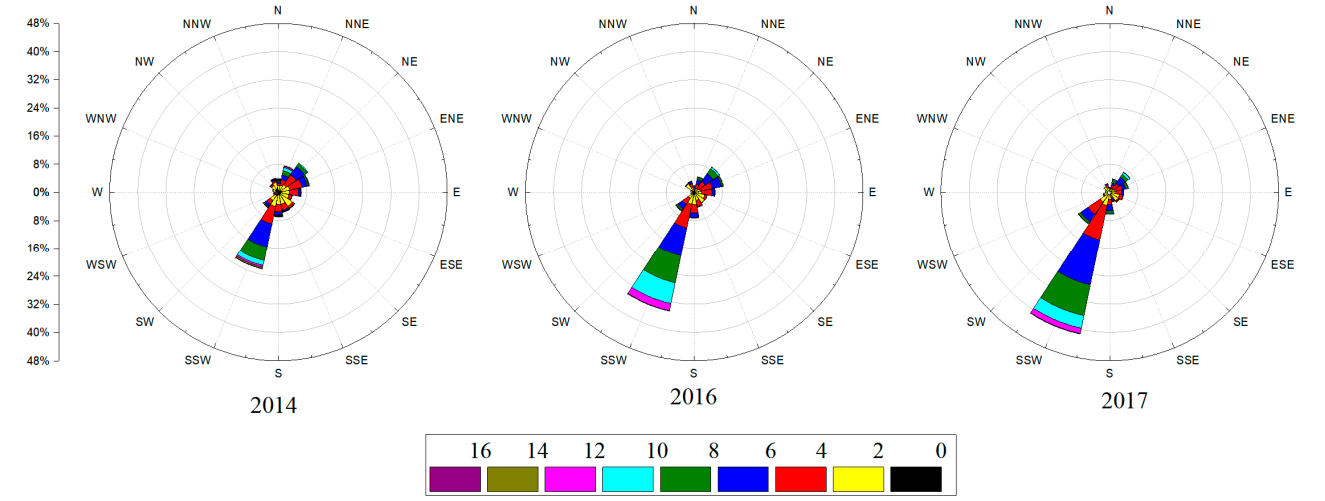

(**b**)

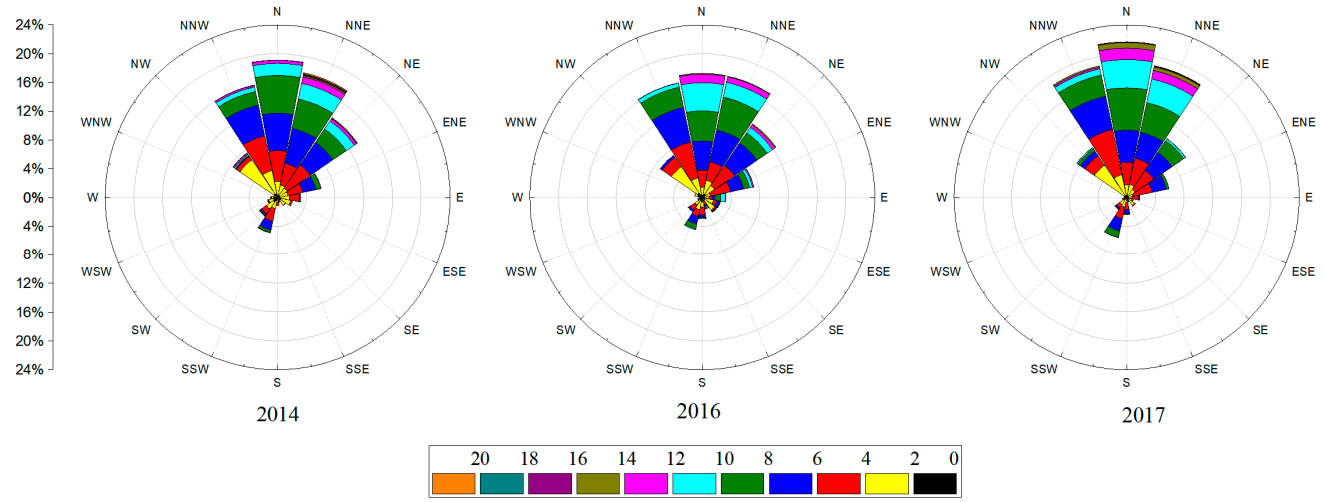

(**c**)

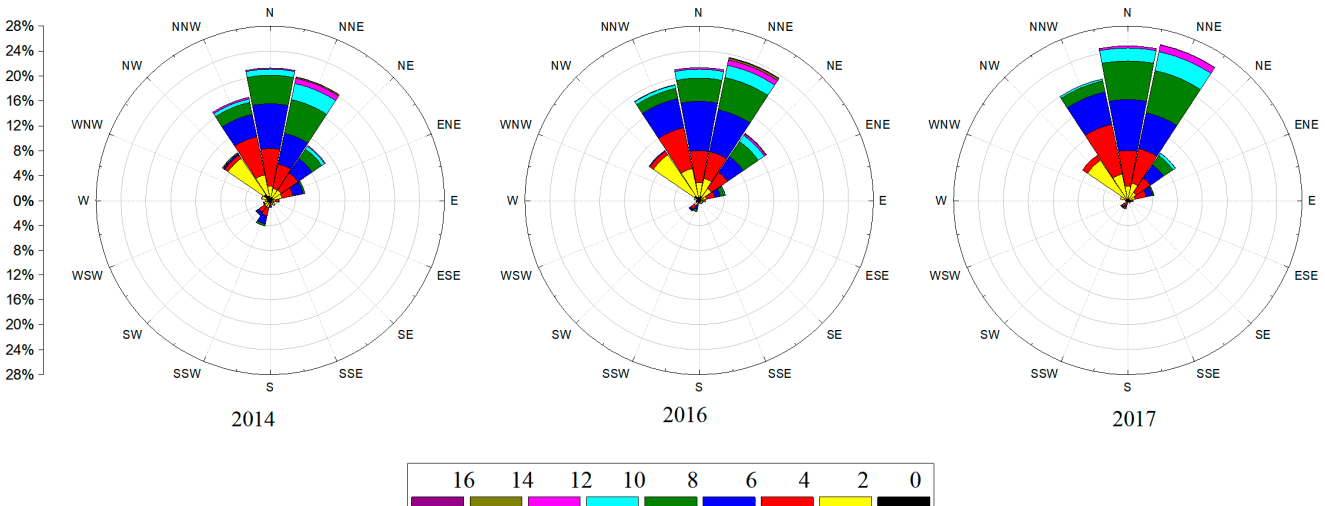

(**d**)

Figure 7. Seasonal wind rose in 3 years: (**a**) spring (March–May); (**b**) summer (June–August); (**c**) autumn (September–November); (**d**) winter (December–February).

4.3. Weibull Parameters and Frequency Histogram

The Weibull shape factor K and scale factor C were obtained by Formulas (4) and (5), and the results are shown in Table 3. As shown in the table, the shape factor K increased continuously from spring to winter in different seasons during the 2016–2017 period. Although it was different in spring and summer in 2014, it still maintained this pattern in autumn and winter. The scale factor C was the highest in autumn, with values of 6.39, 6.95, and 7.33, and it was the lowest in spring, with values of 5.36, 5.32, and 5.24.

Table 3. Seasonal Weibull shape and scale factors.

Site Location	Year	Time	Weibull Shape Factor K	Weibull Scale Factor C
28°25′18.08″ N 121°36′18.29″ E	2014	Spring	1.79	5.36
		Summer	1.73	5.46
		Autumn	2.02	6.67
		Winter	2.14	6.39
	2016	Spring	1.71	5.32
		Summer	2.02	6.37
		Autumn	2.12	6.95
		Winter	2.19	6.55
	2017	Spring	1.91	5.24
		Summer	2.09	6.53
		Autumn	2.28	7.33
		Winter	2.48	6.81

The Weibull distribution curve and the seasonal wind speed frequency histogram for the three years were drawn using the Weibull parameters obtained above (Figure 8). As shown in the figure, the Weibull and frequency distributions of wind speed exhibited high degrees of matching, and thus, the Weibull distribution can be used to evaluate wind energy potential. The histogram of wind speed frequency in Figure 8 presents wind speed frequency in different intervals at intervals of 1 m/s. The difference in frequency at varying wind speeds can be clearly observed by comparing the data. For example, the frequency of the 3-year average wind speed of 2–7 m/s in spring increased continuously, from the lowest value of 63.9% in 2014 to 69.6% in 2017. This increase was also reflected in other seasons. Differences in the same year and various seasons were also recorded. For example, the average wind speed in spring and summer in 2014 was mostly concentrated at 2–7 m/s, while that in autumn and winter was concentrated at 3–10 m/s. In particular, the frequency of the average wind speed at 7–10 m/s increased considerably, from 17.9% in spring to 26% in winter.

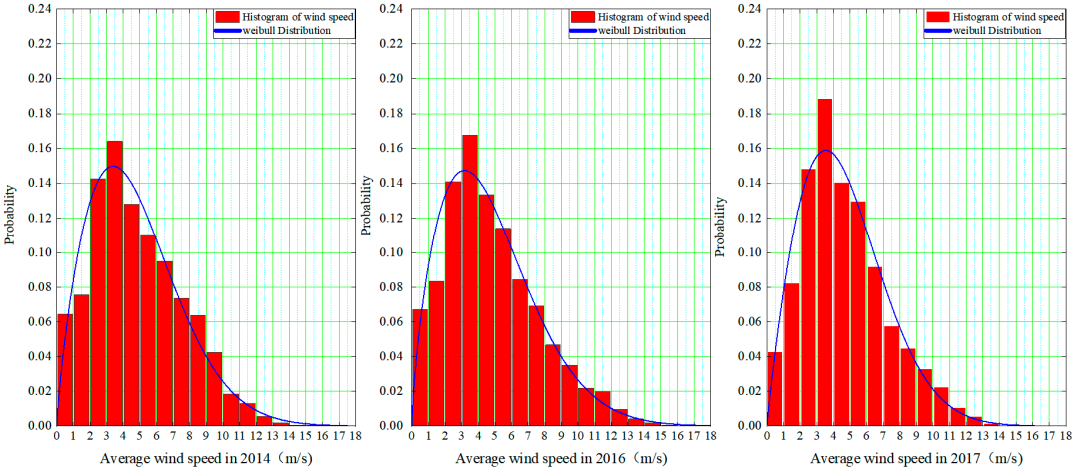

(**a**)

Figure 8. *Cont.*

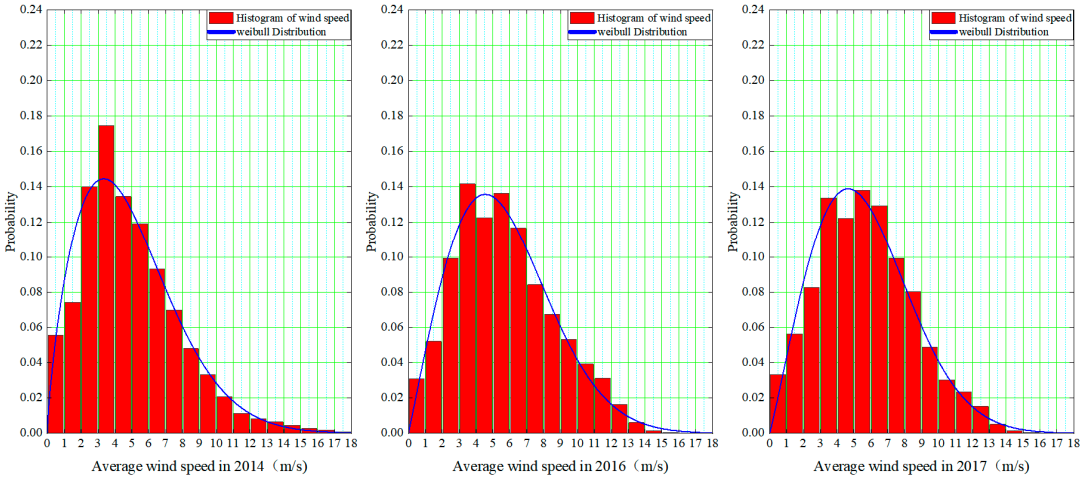

(**b**)

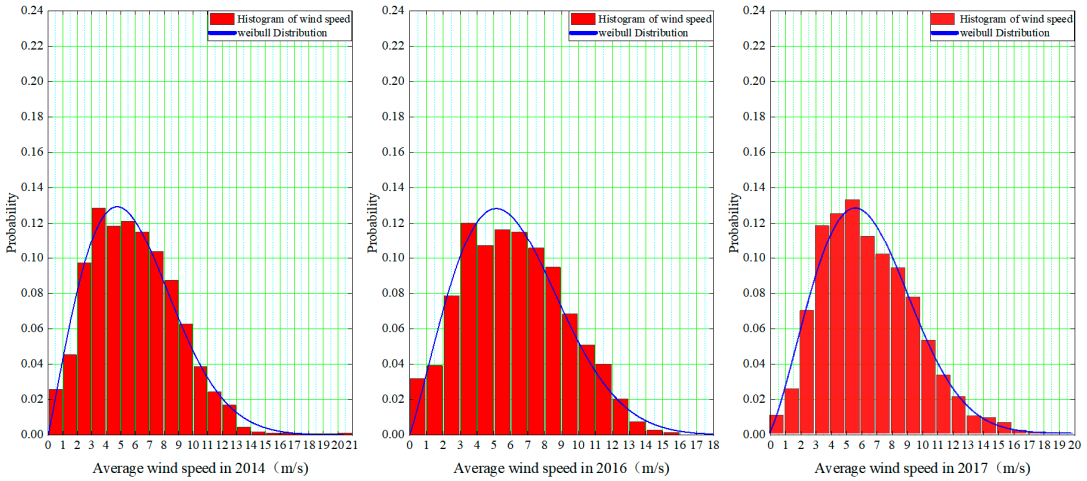

(**c**)

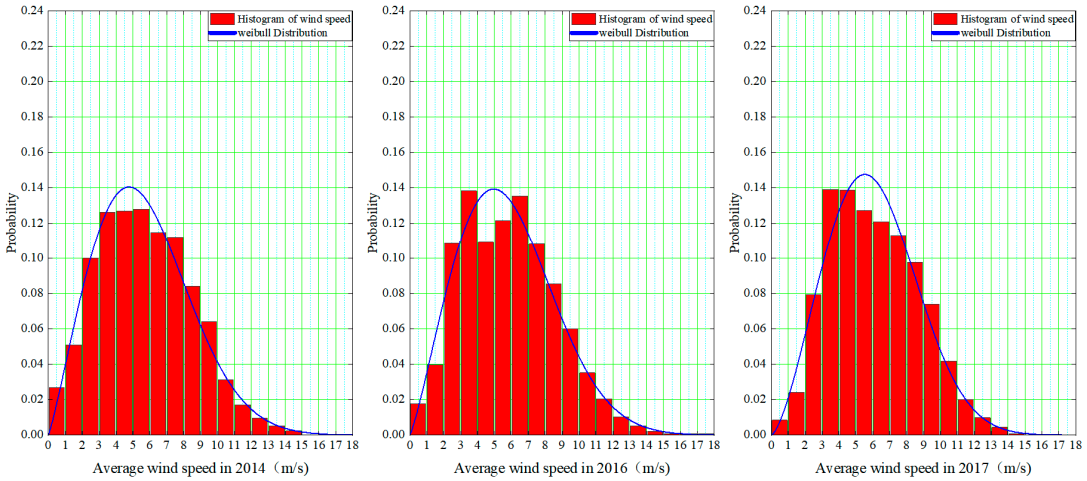

(**d**)

Figure 8. Histogram of seasonal wind speed distribution in 3 years: (**a**) spring (March–May); (**b**) summer (June–August); (**c**) autumn (September–November); (**d**) winter (December–February).

4.4. Wind Energy Density

Wind energy density is the most valuable reference quantity for measuring the amount of wind energy and wind energy reserves in a region. Using Formula (6), the monthly change in wind energy density over the 3 years studied was obtained, as shown in Figure 9.

Comparing Figures 6 and 9 indicates that the monthly variations in average wind speed and wind energy density were the same, and the maximum values appeared in July and October. The wind energy density rates in July were 263, 327, and 293 W/m^2, and the density rates in October were 291, 311, and 424 W/m^2. The minimum values appeared in May, which were 104, 101, and 82 W/m^2. Similarly, the wind speed was low in spring and high in summer and autumn, and the values exhibited obvious seasonal changes. Comparing the 3-year wind energy density data shows that the fluctuation ranges of wind energy density and monthly average wind speed were similar in different years. The wind energy density also varied greatly, especially in July and October, when the average wind speed was the highest. The maximum difference was 133 W/m^2. The abovementioned discussion indicates that the wind energy density and average wind speed in the coastal areas were highly consistent, and wind energy resources were abundant in summer and autumn. However, the fluctuation was large, and the maximum multiple was 1.5 times in different years.

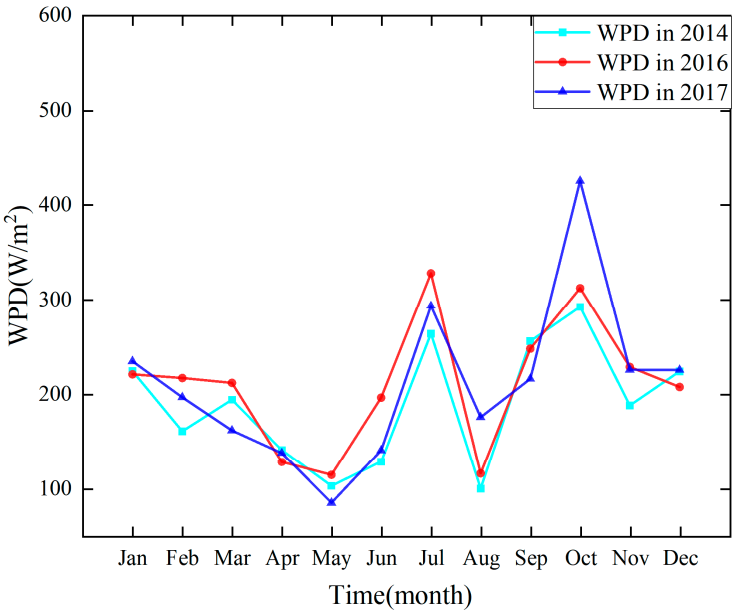

Figure 9. Monthly variation in wind energy density over 3 years.

4.5. Capacity Factor

The theoretical capacity factor is the ratio of the wind turbine's predicted power generation to the rated power generation, wherein the predicted power generation is calculated using Formula (8). In this study, a Vestas® V80/2000 commercial wind turbine was used as an example to calculate the theoretical monthly capacity coefficient of an actual wind farm in this area over three years. The results are presented in Figure 10. The 3-year capacity coefficient of the model V80 wind turbine maintained the same trend as the monthly variation in average wind speed and wind energy density. It was the lowest in May and reached its maximum value in July and October. The values in summer and autumn were significantly higher than those in spring and winter, with noticeable seasonal variation. It also fluctuated considerably in different years in summer and autumn; the maximum value was recorded in October.

The actual capacity factor is the ratio of the actual power generation to the rated power generation of the wind turbine. Table 4 provides the actual power generation of the two wind turbines at different distances from the wind measuring tower in the actual wind farm in 2019 and the monthly capacity coefficient calculated from the actual power generation. The table also presents the monthly operating days of the two wind turbines, which ranged from 15 to 24 days per month. As indicated in the table, the monthly capacity coefficients of the two wind turbines were lower than 0.27 and reached their maximum

value in September and minimum value in June. The maximum values were 0.233 and 0.263, while the minimum values were 0.104 and 0.105.

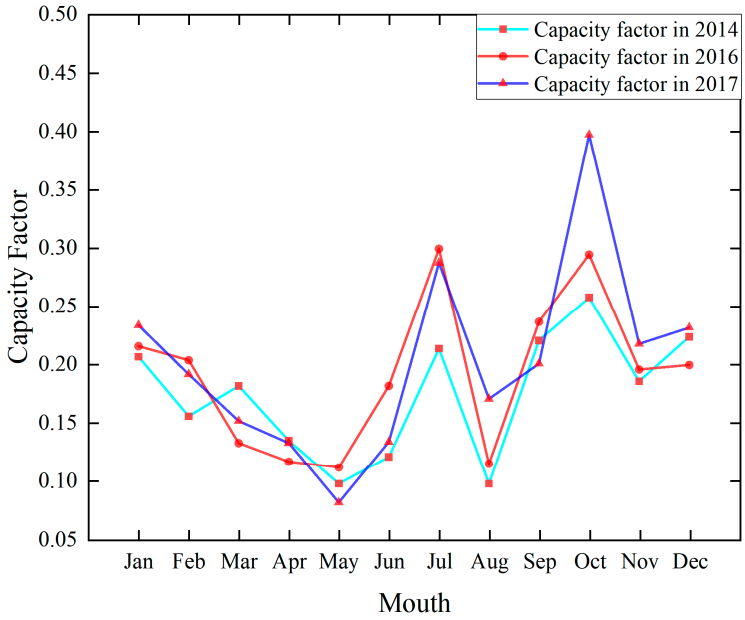

Figure 10. Theoretical capacity factor per month over 3 years.

Table 4. Actual operating days and capacity factor of wind turbines.

Type	Month	Day of Operation in 2019	Capacity Factor in 2019
F1	January	22	0.167
	February	21	0.156
	March	18	0.132
	April	16	0.107
	May	15	0.111
	June	15	0.104
	July	20	0.169
	August	16	0.119
	September	24	0.233
	October	20	0.120
	November	17	0.162
	December	25	0.183
F17	January	20	0.179
	February	20	0.180
	March	20	0.145
	April	16	0.114
	May	17	0.125
	June	15	0.105
	July	20	0.164
	August	18	0.127
	September	25	0.263
	October	20	0.128
	November	23	0.243
	December	24	0.237

4.6. Comparison of Capacity Factors

To better evaluate the accuracy of wind resource prediction in this area, this study compared the relationship between the theoretical capacity factor calculated in three consecutive years and the actual capacity factor of two different wind turbines. The results are presented in Figure 11a,b. As shown in the figure, the changing trend of the actual

capacity coefficient of the F1 wind turbine was basically the same as that of the theoretical capacity coefficient over 3 years, particularly from January to June, August to September, and November to December. The theoretical capacity coefficient was closer to the actual capacity coefficient, and the gap between the theoretical and actual capacity coefficients was excessively large in July and October. The trends ofF17 and F1 wind turbines were similar, and the difference was excessively large in July and October. The theoretical capacity coefficient in other months was close to the actual capacity coefficient, particularly from January to June, and the average difference between them was less than 8%.

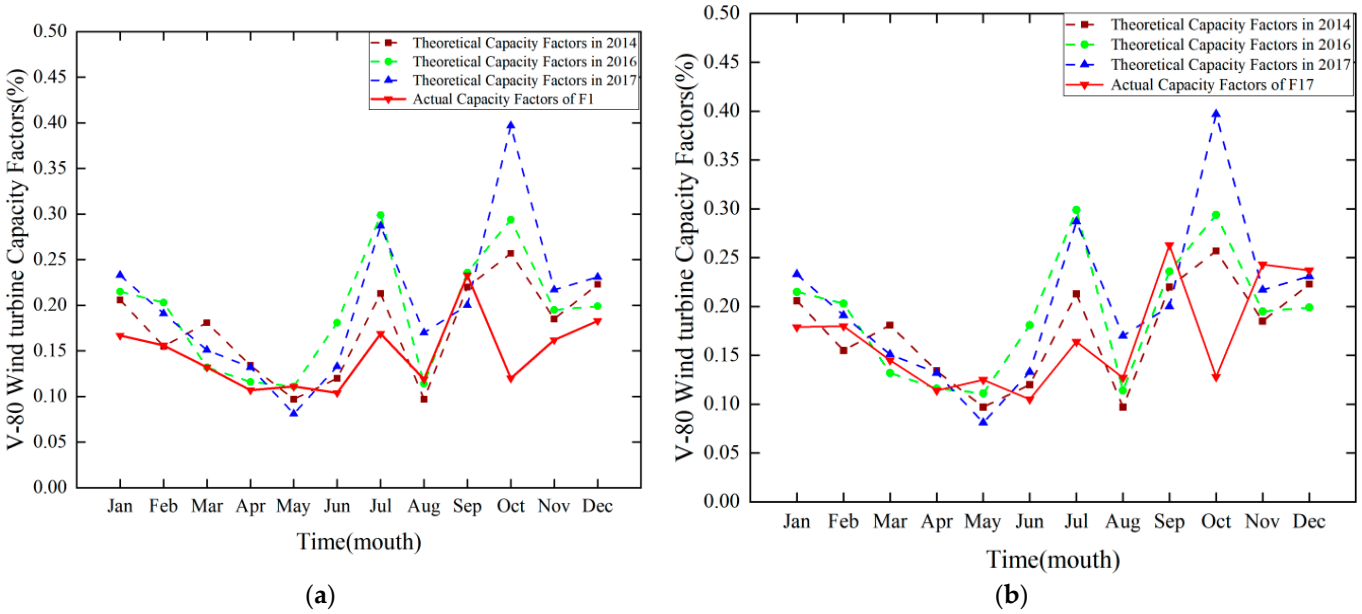

Figure 11. Comparison of actual and theoretical capacity factors: (**a**) F1 and (**b**) F17.

Figure 12 shows the calculated difference between the theoretical capacity factor and the actual capacity factor using Formula (10), clearly illustrating the gap between the predicted and the actual energy generation from the wind. As shown in the figure, the two wind turbines exhibited the same trend. In general, the average difference between the theoretical and actual capacity coefficients was less than 9%, and the difference was more than 9% in July and October, with a maximum value of 28%, which was considerably higher than those in other months. Combined with the monthly average wind speed above, the variation in wind speed during different years was small when the monthly average wind speed was less than 6 m/s. In such a condition, the theoretical and actual capacity coefficients were extremely close, and the prediction was accurate. When the average wind speed in the current month was greater than 6 m/s, the variation range in wind speed in different years increased, the proximity between the theoretical and actual capacity coefficients decreased, and the accuracy of prediction also decreased. Further observation shows that, when considering the actual operation days of wind turbines, the wind energy resources in July and October, with a large difference between theoretical capacity coefficient and actual capacity coefficient, were much higher than those in other months. However, the operation days of wind turbines were lower than those in general months, which may be due to the fact that the complex weather affected the normal operation of the wind turbine.

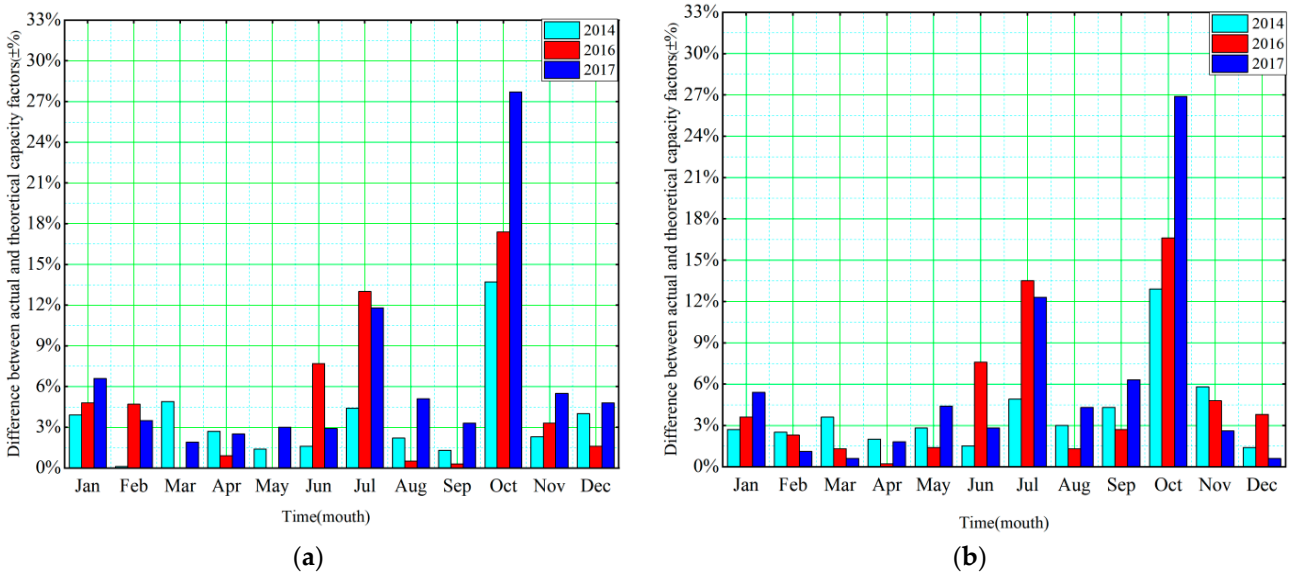

Figure 12. Difference between actual and theoretical capacity coefficients: (**a**) F1 and (**b**) F17.

5. Conclusions

On the basis of the statistical analysis of wind field characteristics, such as average wind speed, Weibull shape and scale factors, wind direction change, and wind energy density, this study compared the predicted capacity coefficient calculated from the wind field data with the actual capacity coefficient calculated from the actual power generation of two wind turbines in a wind farm in the coastal area of Zhejiang Province. The major conclusions drawn include the following findings:

- In terms of the characteristics of wind resources, the 3-year average monthly wind speed and wind energy density in the coastal areas of Zhejiang were basically the same. All indicators were higher in summer and autumn than in spring and winter, with obvious seasonal changes. The results also showed that the monthly average wind speed and wind energy density changed slightly in spring and winter, whereas they changed greatly in summer and autumn, especially in July and October. In this period, the maximum difference in monthly average wind speed was 1.46 times, and the maximum difference in monthly wind energy density was 1.5 times.
- The dominant wind directions during the same season in the 3 years were approximately the same, with obvious seasonal trends. The dominant wind direction in spring was northwesterly, while in summer, it was southwesterly, and in autumn and winter, it was northerly. Wind speed was higher in summer and lower in spring, and wind direction in summer was more concentrated than in other seasons.
- From the comparison of the capacity coefficient, it was deduced that the theoretical capacity coefficient was close to the actual capacity coefficient from January to June, August to September, and November to December, with an average difference of less than 9%, whereas a considerable gap existed between the theoretical and actual capacity coefficient in July and October, with an average difference of more than 9% and a maximum value of 28%. Combined with the monthly average wind speed, the variation in wind speed among different years was small when the monthly average wind speed was less than 6 m/s. In such a condition, the theoretical and actual capacity coefficients were extremely close, and the prediction was accurate. When the average wind speed in the current month was greater than 6 m/s, the variation range of wind speed in different years increased, the proximity between the theoretical and actual capacity coefficients decreased, and the accuracy of prediction also decreased.

In general, the current research shows that although the coastal areas of Zhejiang are rich in wind energy resources, wind energy indicators fluctuate considerably in different years due to the influence of complex weather events, such as typhoons or strong winds, leading to the low accuracy of early wind resource evaluation and, consequently, to the large difference between the estimated wind EO and the actual output capacity of a wind turbine. Therefore, when evaluating the wind energy potential in the coastal areas of Zhejiang, we must consider uncertain and complex weather factors, such as typhoons or strong winds. Using wind farm data from many years is appropriate for evaluation, and the selection of wind turbines must be carefully considered.

Author Contributions: Conceptualization, G.F. and Y.W.; methodology, G.F.; software, G.F.; validation, G.F. and B.Y.; formal analysis, Y.W. and G.F.; investigation, C.Z. and B.F.; resources, Y.W.; data curation, G.F.; writing—original draft preparation, G.F. and Y.W.; visualization, G.F. and Q.Q. All authors have read and agreed to the published version of the manuscript.

Funding: This research was funded by the Zhejiang Province Natural Science Foundation Project (LY19E080022), Natural Science Foundation of China (51508419,51678455), and the Zhejiang Provincial Department of Education Project (The title of the Project: Wind Field Characteristic Monitoring and Wind Load Monitoring Research on Coastal Low-rise Buildings and the number: Y202147409).

Institutional Review Board Statement: Not applicable.

Informed Consent Statement: Not applicable.

Data Availability Statement: Not applicable.

Conflicts of Interest: The authors declare no conflict of interest.

References

1. Wen, Y.; Kamranzad, B.; Lin, P. Assessment of long-term offshore wind energy potential in the south and southeast coasts of China based on a 55-year dataset. *Energy* **2021**, *224*, 120225. [CrossRef]
2. Sawyer, S.; Teske, S.; Fried, L.; Shukla, S. *Global Wind Energy Outlook*; Global Wind Energy Council: Brussels, Belgium, 2016.
3. Liang, Y.; Wu, C.; Ji, X.; Zhang, M.; Li, Y.; He, J.; Qin, Z. Estimation of the influences of spatiotemporal variations in air density on wind energy assessment in China based on deep neural network. *Energy* **2021**, *239*, 122210. [CrossRef]
4. Vestas Leaves Competitors Trailing as Wind Industry Posts Another Record Year of Almost 100 Gigawatts. Available online: https://about.bnef.com/blog/vestas-leaves-competitors-trailing-as-wind-industry-posts-another-record-year-of-almost-100-gigawatts/ (accessed on 10 April 2022).
5. Feng, J.; Feng, L.; Wang, J.; King, C.W. Evaluation of the onshore wind energy potential in mainland China—Based on GIS modeling and EROI analysis. *Resour. Conserv. Recycl.* **2019**, *152*, 104484. [CrossRef]
6. Summary of China's wind power industry operation in 2021 and industry trend forecast in 2022. Available online: https://baijiahao.baidu.com/s?id=1724303810359985333&wfr=spider&for=pc (accessed on 10 April 2022).
7. Chen, X.; Foley, A.; Zhang, Z.; Wang, K.; O'Driscoll, K. An assessment of wind energy potential in the Beibu Gulf considering the energy demands of the Beibu Gulf Economic Rim. *Renew. Sustain. Energy Rev.* **2020**, *119*, 109605. [CrossRef]
8. Shu, Z.; Li, Q.; Chan, P.W. Statistical analysis of wind characteristics and wind energy potential in Hong Kong. *Energy Convers. Manag.* **2015**, *101*, 644–657. [CrossRef]
9. Emeksiz, C.; Demirci, B. The determination of offshore wind energy potential of Turkey by using novelty hybrid site selection method. *Sustain. Energy Technol. Assess.* **2019**, *36*, 100562. [CrossRef]
10. Zhou, W.; Yang, H.; Fang, Z. Wind power potential and characteristic analysis of the Pearl River Delta region, China. *Renew. Energy* **2006**, *31*, 739–753. [CrossRef]
11. Chen, X.; Wang, K.; Zhang, Z.; Zeng, Y.; Zhang, Y.; O'Driscoll, K. An assessment of wind and wave climate as potential sources of renewable energy in the nearshore Shenzhen coastal zone of the South China Sea. *Energy* **2017**, *134*, 789–801. [CrossRef]
12. Deng, G.; Zhang, Z.; Li, Y.; Liu, H.; Xu, W.; Pan, Y. Prospective of development of large-scale tidal current turbine array: An example numerical investigation of Zhejiang, China. *Appl. Energy* **2020**, *264*, 114621. [CrossRef]
13. Li, J.; Yu, X.B. Model and Procedures for Reliable near Term Wind Energy Production Forecast. *Wind Eng.* **2015**, *39*, 595–607. [CrossRef]
14. Kang, S.; Khanjari, A.; You, S.; Lee, J.-H. Comparison of different statistical methods used to estimate Weibull parameters for wind speed contribution in nearby an offshore site, Republic of Korea. *Energy Rep.* **2021**, *7*, 7358–7373. [CrossRef]
15. Safari, B.; Gasore, J. A statistical investigation of wind characteristics and wind energy potential based on the Weibull and Rayleigh models in Rwanda. *Renew. Energy* **2010**, *35*, 2874–2880. [CrossRef]

16. Carta, J.; Ramírez, P.; Velázquez-Medina, S. A review of wind speed probability distributions used in wind energy analysis: Case studies in the Canary Islands. *Renew. Sustain. Energy Rev.* **2009**, *13*, 933–955. [CrossRef]
17. Saleh, H.; Abou El-Azm Aly, A.; Abdel-Hady, S.M. Assessment of different methods used to estimate Weibull distribution parameters for wind speed in Zafarana wind farm, Suez Gulf, Egypt. *Energy* **2012**, *44*, 710–719. [CrossRef]
18. Manwell, J.F.; McGowan, J.G.; Rogers, A.L. *Book Review: Wind Energy Explained: Theory, Design and Application*; John Wiley & Sons: Chichester, UK, 2006; Volume 30, pp. 169–170. [CrossRef]
19. Li, J.; Yu, X.B. LiDAR technology for wind energy potential assessment: Demonstration and validation at a site around Lake Erie. *Energy Convers. Manag.* **2017**, *144*, 252–261. [CrossRef]
20. Gomes, M.S.D.S.; de Paiva, J.M.F.; Moris, V.A.D.S.; Nunes, A.O. Proposal of a methodology to use offshore wind energy on the southeast coast of Brazil. *Energy* **2019**, *185*, 327–336. [CrossRef]
21. Chang, T.P.C. Performance comparison of six numerical methods in estimating Weibull parameters for wind energy application. *Appl. Energy* **2011**, *88*, 272–282. [CrossRef]
22. Usta, I.; Arik, I.; Yenilmez, I.; Kantar, Y.M. A new estimation approach based on moments for estimating Weibull parameters in wind power applications. *Energy Convers. Manag.* **2018**, *164*, 570–578. [CrossRef]
23. Mohammadi, K.; Alavi, O.; Mostafaeipour, A.; Goudarzi, N.; Jalilvand, M. Assessing different parameters estimation methods of Weibull distribution to compute wind power density. *Energy Convers. Manag.* **2016**, *108*, 322–335. [CrossRef]
24. Aukitino, T.; Khan, M.; Ahmed, M.R. Wind energy resource assessment for Kiribati with a comparison of different methods of determining Weibull parameters. *Energy Convers. Manag.* **2017**, *151*, 641–660. [CrossRef]
25. Saeed, M.K.; Salam, A.; Rehman, A.U. Comparison of six different methods of Weibull distribution for wind power assessment: A case study for a site in the Northern region of Pakistan. *Sustain. Energy Technol. Assess.* **2019**, *36*, 100541. [CrossRef]
26. Tizgui, I.; El Guezar, F.; Bouzahir, H.; Benaid, B. Comparison of methods in estimating Weibull parameters for wind energy applications. *Int. J. Energy Sect. Manag.* **2017**, *11*, 650–663. [CrossRef]
27. Ouahabi, M.H.; Elkhachine, H.; Benabdelouahab, F.; Khamlichi, A. Comparative study of five different methods of adjustment by the Weibull model to determine the most accurate method of analyzing annual variations of wind energy in Tetouan—Morocco. *Procedia Manuf.* **2020**, *46*, 698–707. [CrossRef]
28. Sumair, M.; Aized, T.; Bhutta, M.M.A.; Siddiqui, F.A.; Tehreem, L.; Chaudhry, A. Method of Four Moments Mixture-A new approach for parametric estimation of Weibull Probability Distribution for wind potential estimation applications. *Renew. Energy* **2022**, *191*, 291–304. [CrossRef]
29. Wan, J.; Zheng, F.; Luan, H.; Tian, Y.; Li, L.; Ma, Z.; Xu, Z.; Li, Y. Assessment of wind energy resources in the urat area using optimized weibull distribution. *Sustain. Energy Technol. Assess.* **2021**, *47*, 101351. [CrossRef]
30. Saeed, M.A.; Ahmed, Z.; Yang, J.; Zhang, W. An optimal approach of wind power assessment using Chebyshev metric for determining the Weibull distribution parameters. *Sustain. Energy Technol. Assess.* **2019**, *37*, 100612. [CrossRef]
31. Li, J.; Yu, X.B. Onshore and offshore wind energy potential assessment near Lake Erie shoreline: A spatial and temporal analysis. *Energy* **2018**, *147*, 1092–1107. [CrossRef]
32. Khahro, S.F.; Tabbassum, K.; Soomro, A.M.; Dong, L.; Liao, X. Evaluation of wind power production prospective and Weibull parameter estimation methods for Babaurband, Sindh Pakistan. *Energy Convers. Manag.* **2014**, *78*, 956–967. [CrossRef]
33. Carreno-Madinabeitia, S.; Ibarra-Berastegi, G.; Sáenz, J.; Ulazia, A. Long-term changes in offshore wind power density and wind turbine capacity factor in the Iberian Peninsula (1900–2010). *Energy* **2021**, *226*, 120364. [CrossRef]
34. Chen, H.; Anfinsen, S.N.; Birkelund, Y.; Yuan, F. Probability distributions for wind speed volatility characteristics: A case study of Northern Norway. *Energy Rep.* **2021**, *7*, 248–255. [CrossRef]
35. Akdağ, S.A.; Dinler, A. A new method to estimate Weibull parameters for wind energy applications. *Energy Convers. Manag.* **2009**, *50*, 1761–1766. [CrossRef]
36. Guarienti, J.A.; Almeida, A.K.; Neto, A.M.; Ferreira, A.R.D.O.; Ottonelli, J.P.; de Almeida, I.K. Performance analysis of numerical methods for determining Weibull distribution parameters applied to wind speed in Mato Grosso do Sul, Brazil. *Sustain. Energy Technol. Assess.* **2020**, *42*, 100854. [CrossRef]
37. Mahmood, F.H.; Resen, A.; Khamees, A.B. Wind characteristic analysis based on Weibull distribution of Al-Salman site, Iraq. *Energy Rep.* **2019**, *6*, 79–87. [CrossRef]
38. Miao, H.; Dong, D.; Huang, G.; Hu, K.; Tian, Q.; Gong, Y. Evaluation of Northern Hemisphere surface wind speed and wind power density in multiple reanalysis datasets. *Energy* **2020**, *200*, 117382. [CrossRef]
39. Li, Y.; Wu, X.-P.; Li, Q.-S.; Tee, K.F. Assessment of onshore wind energy potential under different geographical climate conditions in China. *Energy* **2018**, *152*, 498–511. [CrossRef]
40. Quan, P.; Leephakpreeda, T. Assessment of wind energy potential for selecting wind turbines: An application to Thailand. *Sustain. Energy Technol. Assess.* **2015**, *11*, 17–26. [CrossRef]
41. Wilkie, D.; Galasso, C. A Bayesian model for wind farm capacity factors. *Energy Convers. Manag.* **2021**, *252*, 114950. [CrossRef]